VOL. 84, NO. B1 JOURNAL OF GEOPHYSICAL RESEARCH JANUARY 10, 1979

VELOCITY ANISOTROPY IN SEMI-INDURATED CALCAREOUS DEEP SEA SEDIMENTS

R. L. Carlson[1] and N. I. Christensen

Department of Geological Sciences, University of Washington, Seattle, Washington 98195

Abstract. Compressional-wave velocities have been measured for propagation directions parallel and perpendicular to bedding in 11 calcareous deep sea sediments at confining pressures to 1.0 kbar. The samples, recovered from subbottom depths of 0.39-0.75 km in the western South Atlantic on DSDP leg 39, range in wet bulk density from 1.83 to 2.30 g/cm^{-3} and in porosity from 23 to 48%. The sediments exhibit significant velocity anisotropy at all pressures, with velocities in the bedding plane higher than those measured in the vertical direction. At 0.1 kbar, horizontal velocities (V_h) range from 1.80 to 2.99 km/s, while vertical velocities range from 1.65 to 2.54 km/s. Corresponding ranges of $\Delta V = (V_h - V_v)$ and anisotropy ($A = 2(V_h - V_v)/(V_h + V_v)$) are 0.10-0.45 km/s and 5.2-16.3%, respectively. Both ΔV and A increase markedly with depth of burial: $\partial \Delta V / \partial z = 0.62$ km/s/km, and $\partial A / \partial z = 19\%$/km. The failure of anisotropy to decrease with increasing confining pressure suggests that this phenomenon is not produced by the alignment of cracks. However, the elastic properties of calcite are such that an alignment of *c* axes perpendicular to bedding would produce the observed velocity distribution. Suggested mechanisms for producing the fabric are: (1) the alignment of certain microfossils such as Discoaster during compaction, (2) epitaxial growth of aligned forms during diagenesis, and (3) recrystallization of calcite.

Introduction

Laboratory observations of seismic anisotropy reflect a preferred orientation of cracks and/or mineral grains in the sample. Anisotropy has been observed by several investigators [eg., Boyce, 1976; Tucholke et al., 1976] in studies of compressional-wave velocities in sediments recovered by the Deep Sea Drilling Project (DSDP), but because the measurements were made at atmospheric pressure it is not clear whether the velocity anisotropy will persist at in situ pressures. The few velocity measurements which have been made at elevated pressures [e.g. Schreiber et al., 1972; Christensen et al., 1973] suggest that significant anisotropy is present in some calcareous rocks.

Calcareous sediments are among those most frequently recovered by deep sea drilling, and their widespread occurrence and significance are well documented [e.g., Heezen et al., 1973; van Andel, 1974]. Thus if velocity anisotropy is pervasive in sections containing abundant calcareous sediments, it will be an important factor influencing the propagation of seismic waves in the uppermost regions of the oceanic crust. For example, the variable-angle reflection method is commonly used to determine the velocity structure of the deep sea sediment column [e.g., Houtz et al., 1978, 1970; Hamilton et al., 1974; 1977], and because the data reduction technique assumes the sediments to be elastically isotropic [Dix, 1955; Clay and Rona, 1965; Le Pichon et al., 1968], the presence of marked velocity anisotropy may introduce significant errors in velocity and depth determinations.

The purpose of this study is to investigate velocity anisotropy in semi-indurated calcareous deep-sea sediments at in situ pressures. We have selected a variety of samples for measurement, collected at different depths from three sites in the western South Atlantic on leg 39 of the Deep Sea Drilling Project. The study originated as part of a preliminary investigation of seismic velocities in rocks from the South Atlantic [Carlson and Christensen, 1977a, b].

Procedures

Water saturation and porosity have long been recognized as significant factors affecting the elastic properties of rocks [Wyllie et al., 1985; Nur and Simmons, 1969; Hamilton, 1971]. To retain maximum water saturation, all samples discussed in this paper were shipped to the shore laboratory in sealed, water-filled containers, and saturation was carefully maintained until all measurements were completed.

Another very important consideration is the extent to which the cores have been disturbed by drilling, because the physical properties of disturbed sediments clearly cannot be related to conditions within the sediment column. None of the samples used in this study showed any evidence of drilling disturbance. Bedding was plainly visible in each core and showed no indication of distortion. Moreover, subjecting the samples to confining pressures of 1.0 kbar produced no significant change in length or diameter.

Two samples in the form of right circular cylinders, 2.54 cm in diameter and 2.9-3.8 cm in length, were cut from adjacent parts of 11 DSDP core sections. The cylinders were cut with axes parallel and perpendicular to the core axis to facilitate the measurement of compressional-wave velocities parallel and perpendicular to bedding. Because the water-saturated samples proved to be easily damaged in handling, density and porosity measurements were made using wafers 0.5-1.0 cm thick trimmed from the ends of the horizontal cylinders. After wet-bulk densities were determined by immersion, the samples were weighed to the nearest 0.01 g. Sample volumes were then computed from the weights and densities. Finally, the wafers were air dried and weighed again in order to determine water contents and porosities. No correction

[1]Present Address: Department of Geophysics, Texas A&M University, College Station, Texas 77843.

TABLE 1. Summary of Physical Properties

Sample	ρ	ϕ	d	P	V_h	V_v	ΔV	A	Lith
345-12-0(1)	1.92	42	0.605	0.1	2.11	1.97	0.14	6.9	zeolitic, marly,
				0.2	2.15	2.00	0.15	7.2	diatomaceous
				0.4	2.20	2.06	0.14	6.6	nannochalk
				0.6	2.25	2.12	0.13	5.9	
				0.8	2.30	2.17	0.13	5.8	
				1.0	2.35	2.21	0.14	6.1	
354-14-0(2)	2.02	35	0.700	0.1	2.61	2.41	0.20	8.0	marly
				0.2	2.64	2.43	0.21	8.3	nannochalk
				0.4	2.68	2.44	0.24	9.4	
				0.6	2.73	2.50	0.23	8.8	
				0.8	2.79	2.56	0.23	8.6	
				1.0	2.85	2.62	0.23	8.4	
356-27-0(3)	1.83	48	0.390	0.1	1.80	1.65	0.15	8.7	foram
				0.2	1.83	1.68	0.15	8.5	nannochalk
				0.4	1.87	1.72	0.15	8.4	
				0.6	1.91	1.77	0.14	7.6	
				0.8	1.95	1.81	0.14	7.4	
				1.0	1.99	1.85	0.14	7.3	
356-30-0(4)	1.96	41	0.420	0.1	1.92	1.82	0.10	5.3	foram
				0.2	1.96	1.85	0.11	5.8	nannochalk
				0.4	2.02	1.90	0.12	6.1	
				0.6	2.07	1.95	0.12	6.0	
				0.8	2.12	2.00	0.12	5.8	
				1.0	2.14	2.04	0.10	4.8	
356-35-0(5)	2.18	28	0.540	0.1	2.47	2.25	0.22	9.3	dolomitic, marly,
				0.2	2.53	2.29	0.24	10.0	calcareous chalk
				0.4	2.62	2.35	0.27	10.9	
				0.6	2.66	2.41	0.25	9.9	
				0.8	2.68	2.46	0.22	8.6	
				1.0	2.68	2.51	0.17	6.6	
356-40-0(6)	2.19	29	0.690	0.1	2.43	2.19	0.24	10.4	calcareous
				0.2	2.47	2.22	0.25	10.7	mudstone
				0.4	2.54	2.28	0.26	10.8	
				0.6	2.59	2.34	0.25	10.1	
				0.8	2.65	2.40	0.25	9.9	
				1.0	2.70	2.45	0.25	9.7	
356-43-0(7)	2.30	24	0.720	0.1	2.99	2.54	0.45	16.3	marly
				0.2	3.05	2.59	0.46	16.3	limestone
				0.4	3.14	2.68	0.46	15.8	
				0.6	3.21	2.73	0.48	16.2	
				0.8	3.28	2.79	0.49	16.1	
				1.0	3.35	2.84	0.51	16.5	
357-26-0(8)	2.00	41	0.375	0.1	1.96	1.86	0.10	5.2	limestone
				0.2	1.99	1.90	0.09	4.6	
				0.4	2.04	1.96	0.08	4.0	
				0.6	2.10	2.01	0.09	4.4	
				0.8	2.14	2.05	0.09	4.3	
				1.0	2.17	2.09	0.08	3.8	
357-34-0(9)	2.04	40	0.550	0.1	2.06	1.92	0.14	7.0	foram
				0.2	2.09	1.95	0.14	6.9	nannochalk
				0.4	2.15	2.01	0.14	6.7	
				0.6	2.21	2.07	0.14	6.5	
				0.8	2.28	2.12	0.16	7.3	
				1.0	2.33	2.16	0.17	7.6	
357-43-0(10)	2.13	31	0.720	0.1	2.46	2.13	0.33	14.4	marly, foram
				0.2	2.51	2.16	0.35	15.0	nannochalk
				0.4	2.57	2.21	0.36	15.1	

TABLE 1. (continued)

Sample	ρ	φ	d	P	V_h	V_v	ΔV	A	Lith
				0.6	2.62	2.26	0.36	14.8	
				0.8	2.66	2.31	0.35	14.1	
				1.0	2.71	2.36	0.35	13.8	
357-47-0(11)	2.30	23	0.750	0.1	2.82	2.48	0.34	12.8	marly chalk
				0.2	2.84	2.53	0.31	11.5	
				0.4	2.85	2.59	0.26	9.6	
				0.6	2.96	2.65	0.31	11.1	
				0.8	2.98	2.72	0.26	9.1	
				1.0	3.00	2.78	0.22	7.6	

Parameter ρ is wet-bulk density in g/cm^3;
φ is porosity in 0/0;
d is depth of burial in km;
P is confining pressure in kilobars;
V_h is velocity parallel to bedding in km/s;
V_v is velocity perpendicular to bedding in km/s;
ΔV is V_h-V_v in km/s;
A is anisotropy in 0/0.

was made for the salinity of the pore fluid. The calculated porosities are accurate to ±4%, provided the samples were completely water saturated.

Compressional-wave velocities were measured by the pulse-transmission method as described by Birch [1960], at hydrostatic confining pressures to 1.0 kbar. Though the accuracy of this technique is 0.5% at pressures above a few kilobars [Christensen and Shaw, 1970], an error value of 2% is perhaps more realistic for confining pressures less than 1.0 kbar. Prior to the pressure runs the sides of the cylinders were wrapped in two layers of 100-mesh copper screen and enclosed in copper foil, and the ends of the samples were sealed with silver-conducting paint. The purpose of the screen is to maintain pore pressures substantially lower than the confining pressure by providing voids into which pore water can escape. The foil prevents the pressure medium from penetrating the rock, and with the conducting paint, provides an electrical ground for the transducers. Electrodes having the same diameter as the samples were held in place with gum-rubber tubing, which prevents the pressure medium from entering the space between the transducer and the sample or entering the sample through the ends.

Results

Wet-bulk densities, porosities, depths of recovery, velocity-pressure data, anisotropy data, and brief sample descriptions are listed in Table 1. Sample numbers refer to DSDP site, core, and section. Numbers in parentheses are arbitrarily assigned and correspond to the numbers shown in Figures 1 and 3-7. V_h refers to the velocities of compressional waves propagating in the horizontal direction. Similarly, V_v refers to waves propagating in the vertical direction, and anisotropy is expressed as

$$A(\%) = 2(V_h - V_v)/(V_h + V_v) \times 100 \qquad (1)$$

Of particular importance in this discussion are relations between anisotropy A and other parameters: mean velocity $\bar{V}$, density ρ, porosity φ, and depth of burial d; density-porosity and velocity-density relations are also of interest.

Wet-bulk density values for this suite of calcareous sediments range from 1.8 to 2.3 g/cm^3, with corresponding porosities ranging from 48 to 23%. The relationship between ρ and φ is graphically illustrated in Figure 1. A linear least squares fit on ρ on φ (where φ is factional porosity) produced the relation

$$\rho(g/cm^3) = 2.71 - 1.82\phi \qquad (2)$$

with a correlation coefficient r of 0.98. Thus these samples have a uniform grain density near 2.7 g/cm^3. This result is in excellent agreement with previous observations based upon large numbers of samples [Hamilton, 1970]. However, the implied pore fluid density of 0.89 g/cm^3 suggests that these sediments were either slightly undersaturated at the time of measurement or that some water was trapped in pore spaces after drying.

Sediment compressional-wave velocities, measured parallel and perpendicular to bedding at 0.5 kbar, are plotted against density in Figure 2. Similar data for oceanic DSDP basalts [Christensen and Salisbury, 1975] are included for comparison. As expected, compressional-wave velocities increase with increasing sample density, but the sediment velocities are 1.0-1.5 km/s lower than the velocities of oceanic basalts having similar densities. A remarkable degree of velocity anisotropy is also apparent in Figure 2. Velocities in the horizontal direction are higher than those in the vertical direction, a result which is consistent with measurements made at atmospheric pressure

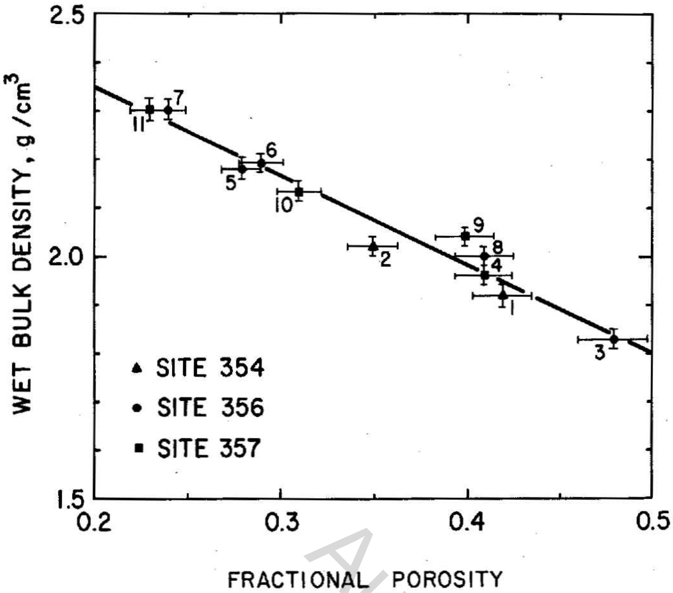

Fig. 1. Wet-bulk density versus fractional porosity. Error bars are computed assuming a 1% error in density and an error of 4% in porosity. Numbers correspond to those listed in Table 1. The regression equation is $\rho = 2.71(\pm 0.04) - 1.82(\pm 0.13)\phi$.

[Boyce, 1976; Tucholke et al., 1976]. Also evident is the tendency for anisotropy to increase with increasing density or increasing mean velocity.

The relationships of anisotropy to average velocity $\overline{V}$ at 0.1 kbar and to density ρ are illustrated in Figures 3 and 4, respectively. In each case a linear regression equation has been computed, with correlation coefficients of 0.75. Anisotropy is seen to increase markedly with mean velocity or density. The range of anisotropy values is 5.2-16.3%.

The variation of anisotropy at 0.1 kbar with depth of sample recovery is illustrated in Figure 5; the same point is illustrated in Figure 6, but the difference in velocities, $\Delta V = V_h - V_v$ measured at 0.1 kbar, has been used to give the reader a feeling for the magnitude of the velocity anisotropy in kilometers per second. The range of recovery depths is 0.39-0.75 km. The figures show that velocity anisotropy is well developed at depths of burial less than 0.4 km and that anisotropy increases markedly with depth, the rate of increase of ΔV being 0.62 ± 0.16 km/s/km.

Discussion

Several pertinent points regarding the occurrence of velocity anisotropy in calcareous deep sea sediments are evident. With values in excess of 5%, velocity anisotropy is strongly in evidence at depths of burial less than 0.4 km. Between 0.4 and 0.8 km, anisotropy increases approximately 19%/km and reaches a value near 16% at the lowest level sampled (Figure 5). The rate of increase in the difference between horizontal and vertical velocities is 0.62 ± 0.16 km/s/km, with a maximum difference between V_h and V_v of 0.45 km/s.

A particularly important point is that the samples used in this study were recovered at DSDP sites 354, 356, and 357, in water depths of 4045, 3175, and 2086 m respectively. The addition of water depths to the depths of overburden shown in Figures 5 and 6 introduces a large degree of scatter. Hence velocity anisotropy in calcareous sediments is closely related to depth of overburden, but bears little relationship to depth below sea level.

In the absence of optical or X ray petrofabric data the specific causes of velocity anisotropy in these calcareous sediments remain unknown, but there are at least two possible causes: (1) the alignment of cracks and pores in bedding planes and (2) preferred orientation of calcite resulting from either mechanical or chemical processes. Two lines of evidence suggest that the geometry of cracks and pores is not responsible for the observed velocity anisotropy in calcareous sediments. Because pore spaces close under increasing pressure, vertical velocities would be expected to increase more rapidly than horizontal velocities with depth, producing a decrease in anisotropy. In fact,

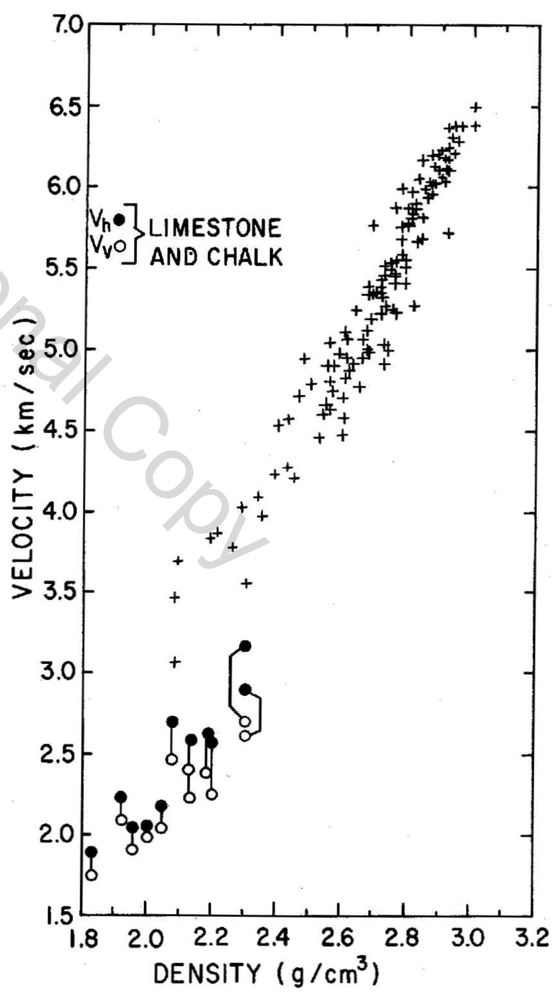

Fig. 2. Wet-bulk density versus velocity measured at 0.5 kbar. Open circles are sediment velocities measured normal to bedding; solid circles represent velocities measured parallel to bedding. Crosses represent DSDP basalt data from Christensen and Salisbury [1975].

anisotropy increases with increasing depth of overburden, as discussed above. Furthermore, if the observed anisotropy were caused by the alignment of pore spaces, anisotropy would decrease with increasing confining pressure applied to a particular sample. In Figure 7, ΔV is plotted against confining pressure. In 9 of the 11 cases studied, confining pressure is seen to have no appreciable effect on the difference between the velocity in the bedding plane and the velocity normal to bedding.

Peselnick and Robie [1962] and Dandekar [1968] have measured compressional-and shear-wave velocities in calcite single crystals at atmospheric pressure. Dandekar [1968] found that the compressional-wave velocity for propagation parallel to the *c* crystallographic axis is 5.61 km/s, while the velocity of propagation in the plane normal to the *c* axis is about 7.35 km/s. Thus a preferred orientation of calcite grains with *c* axes perpendicular to bedding planes would produce the anisotropy pattern observed in this study. The development of such a fabric presents a complex problem.

Calcareous deep sea sediments consist almost exclusively of biogenic detritus, the calcareous remains of microfossils which accumulate on the sea floor. The highly ordered arrangement of calcite crystallites which make up certain forms including those of the Coccolithus pelagicus group, the Cyclococcolithus leptoporus group, and the Discoasters is such that the optic axes of the calcite crystals are normal to the long dimensions of the microfossils (S. Gartner, personal communication, 1977). Other coccoliths are also known to have well ordered structures [Black, 1963; Bukry, 1971], but in these forms of calcite *c* axes are not perpendicular to their long dimensions, and the geometric details of their structures are poorly understood. Though they appear to be randomly oriented in oozes, under compaction, such disclike forms should align themselves with the bedding planes, thereby tending to align the calcite *c* axes normal to bedding.

The fabric initially produced by compaction is likely to be enhanced by epitaxial growth. Simultaneous dissolution and reprecipitation are known to occur during carbonate diagenesis [e.g., van der Lingen and Packham, 1975; Schlanger and Douglas, 1974; Packham and van der Lingen, 1973]. Bain [1940] concluded that faces nearly perpendicular to the *c* axis in

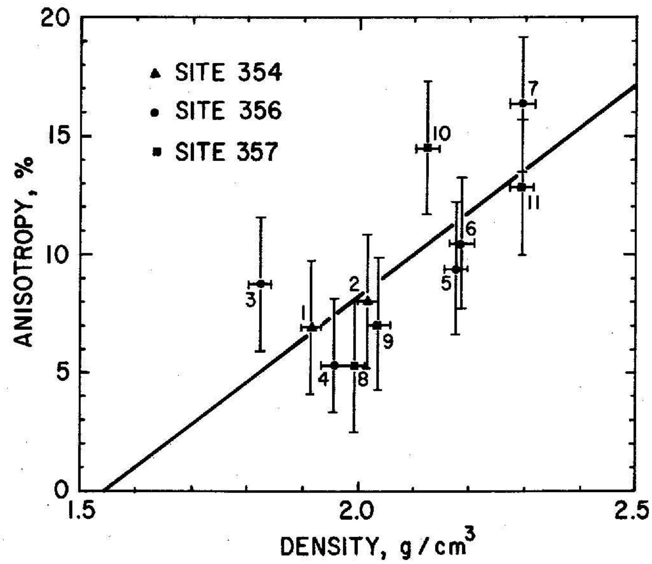

Fig. 4. Anisotropy at 0.1 kbar versus wet-bulk density. Error bars are based on a 2.0% error in measured velocity and a 1.0% error in density. Numbers correspond to those listed in Table 1. The regression equation is $A = 17.74(\pm 5.28)\rho - 27.41(\pm 11.01)$.

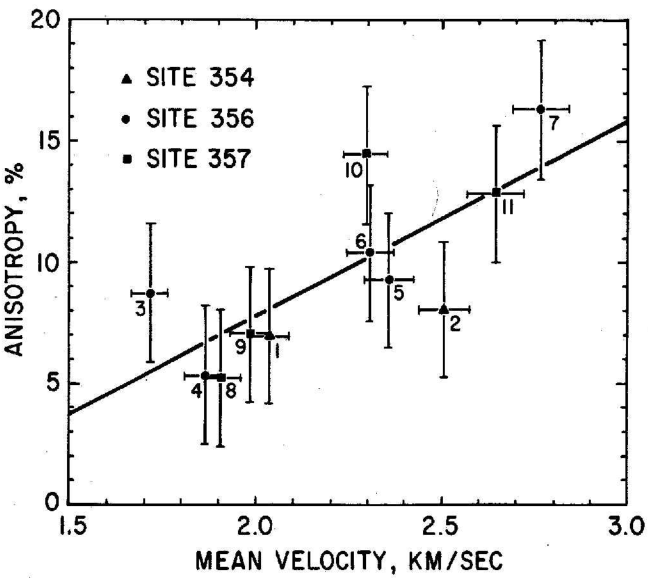

Fig. 3. Anisotropy at 0.1 kbar versus average velocity measured at 0.1 kbar. Error bars are computed assuming a 2.0% error in measured velocity. The regression equation is $A = 8.07(+2.35)\bar{V} - 8.46\ (\pm 5.27)$. Numbers shown correspond to those listed in Table 1.

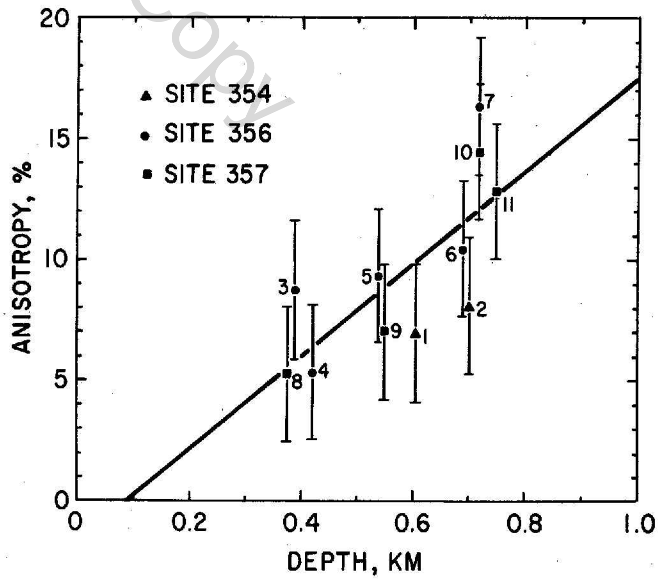

Fig. 5. Anisotropy at 0.1 kbar versus sub-bottom depth of recovery. Error bars are computed assuming a 2.0% error in velocity. Numbers correspond to those listed in Table 1. The regression equation is $A = 19.07(\pm 5.78)d - 1.72(+3.49)$.

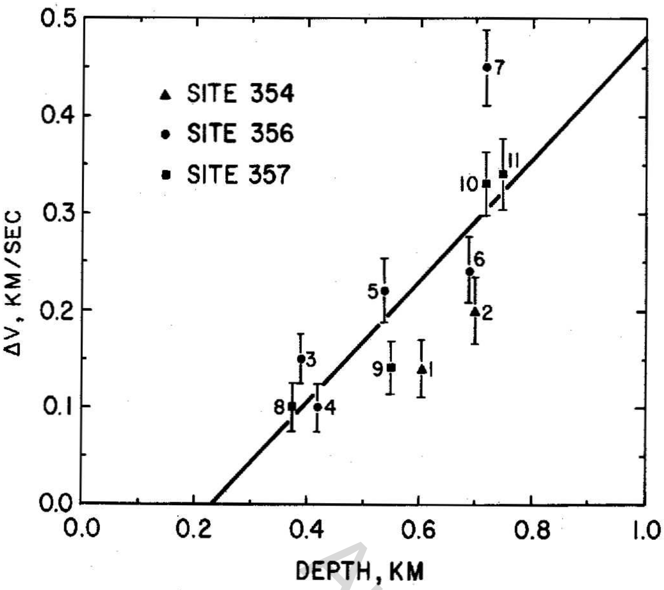

Fig. 6. Velocity difference ($\Delta V = V_h - V_v$) at 1.0 kbar versus depth of sample recovery. Error bars are computed assuming a 2.0% error in measured velocity. Numbers correspond to those listed in Table 1. The regression equation is $\Delta V = 0.62(\pm 0.16)d - 0.15(\pm 0.10)$.

calcite are more resistant to dissolution than those more nearly parallel to *c*, and Bukry [1971] has observed that forms most resistant to solution are those with *c* axes normal to their long dimensions. Indeed, such forms are those on which reprecipitation commonly occurs. For example, Adelseck et al. [1963] and van der Lingen and Packham [1975] have observed that reprecipitation commonly occurs first on Discoasters. These observations imply that the preferred orientation of calcite grains in calcareous sediments may be enhanced during diagenesis by the process

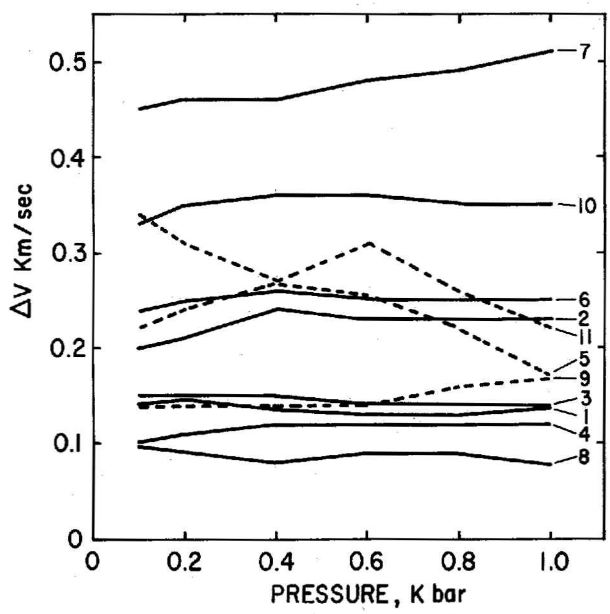

Fig. 7. Velocity difference ($\Delta V = V_h - V_v$) versus confining pressure for each sample studied. Numbers correspond to those listed in Table 1.

of epitaxial growth, that is, by the growth of forms having *c* axes perpendicular to bedding at the expense of smaller, less resistant microfossils and fragments. A mechanism of this kind would also help to account for the fact that velocity anisotropy increases with depth of burial.

Finally, there remains the possibility of calcite recrystallization. Studies by Griggs et al. [1960], Heard [1963], Ferreira and Turner [1964], Friedman [1964], and Neumann [1969] have shown that calcite recrystallization produces a strong fabric with *c* axes normal to the extension directions, in this case the bedding plane. Furthermore, the temperature required to initiate recrystallization in calcite is found to be inversely related to strain rate. Whether conditions at depth in the sediment column will produce calcite recrystallization is unknown, but if this process does operate, it will produce a fabric which is compatible with the observed velocity anisotropy.

Acknowledgements. We wish to thank S. Gartner, A. F. Gangi, and D. A. Fahlquist for their many helpful suggestions and for critically reviewing the manuscript. We also wish to thank V. Kiefer, J. Hull, J. Willemin, and K. Hubert for technical assistance. Financial support was provided by Office of Naval Research contract N-00014-0502. Contribution of the Texas A&M Geodynamics Research Program 2.

References

Adelseck, C. G., G. W. Geeham, P. H. Roth, Experimental evidence for the selective dissolution and overgrowth of calcareous nannofossils during diagenesis, Geol. Soc. Amer. Bull., 84, 2755, 1973.

Bain, G. W., Geological, chemical and physical problems in the marble industry, Tech. Publ. 1261, 16 pp., Amer. Inst. of Mining and Met. Eng., New York, 1940.

Birch, F., The velocity of compressional waves in rocks to 10 kilobars, 1, J. Geophys. Res., 65, 1083, 1960.

Black, M., The fine structure of the mineral parts of Coccolithophidae, Proc. Linn. Soc. London, 1974, 1963.

Boyce, R. E., Sound velocity-density parameters of sediments and rocks from DSDP Sites 315-318 on the Line Islands, Manihiki Plateau, and Tuamotu Ridge in the Pacific Ocean, in Initial Reports of the Deep Sea Drilling Project, vol. 33, edited by S. O. Schlanger et al., p. 685, U. S. Government Printing Office, Washington, D. C., 1976.

Bukry, D., Cenozoic calcareous nannofossils from the Pacific Ocean, Trans. San Diego Soc. Nat. Hist., 16, 303, 1971.

Carlson, R. L., and N. I. Christensen, Velocity anisotropy and physical properties of deep-sea sediments from the western South Atlantic, in Initial Reports of the Deep Sea Drilling Project, vol. 39, edited by P. R. Supro et al., p. 555, U. S. Government Printing Office, Washington, D. C., 1977a.

Carlson, R. L., and N. I. Christensen, Velocities, densities and elastic constants of basalt and trachytic tuff, DSDP leg 39, in Initial Reports of the Deep Sea Drilling Project, vol. 39, edited by P. R. Supro, p. 493, U. S. Government Printing Office, Washington, D. C., 1977b.

Christensen, N. I., and M. H. Salisbury, Structure and constitution of the lower oceanic crust, Rev. Geophys. Space Phys., 13 57, 1975.

Christensen, N. I., and G. H. Shaw, Elasticity of mafic rocks from the Mid-Atlantic Ridge, Geophys. J. Roy. Astron. Soc., 20, 271, 1970.

Christensen, N. I., D. M. Fountain, and R. J. Stewart, Oceanic crustal basement: A comparison of seismic properties of DSDP basalts and consolidated sediments, Mar. Geol., 15 215, 1973.

Clay, C. S., and P. A. Rona, Studies of seismic reflections from thin layers on the ocean bottom in the western North Atlantic, J. Geophys. Res., 70, 855, 1965.

Dandekar, D. P., Elastic constants of calcite, J. Appl. Phys., 39, 2971, 1968.

Dix, C. H., Seismic velocities from surface measurements, Geophysics, 20, 68, 1955.

Ferreira, M. P., and F. J. Turner, Microscopic structure and fabric of Yule marble experimentally deformed at different strain rates, J. Geol., 72, 861, 1964.

Friedman, M., Petrofabric techniques for the determination of principle stress directions in rocks, in State of Stress in the Earth's Crust, edited by W. R. Judd, p. 451, Elsevier, New York, 1964.

Griggs, D. T., F. J. Turner and H. C. Heard, Deformation of rocks at 500° to 800°C, Geol. Soc. Amer. Mem., 79, 39, 1960.

Hamilton, E. L., Sound velocity and related properties of marine sediments, North Pacific, J. Geophys. Res., 75, 4423, 1970.

Hamilton, E. L., Elastic properties of marine sediments, J. Geophys. Res., 76, 579, 1971.

Hamilton, E. L., D. G. Moore, E. Buffington, P. Sherrer, and J. R. Curray, Sediment velocities from sonobuoys: Bay of Bengal, Bering Sea, Japan Sea, and North Pacific, J. Geophys. Res., 79, 2653, 1974.

Hamilton, E. L., R. T. Bachman, J. R. Curry, and D. G. Moore, Sediment velocities from sonobuoys: Bengal Fan, Sunda Trench, Andamin Basin, and Nicobar Fan, J. Geophys. Res., 82, 3003, 1977.

Heard, H. C., Effects of large changes in strain rate on deformation of Yule marble, J. Geol., 71, 1962, 1963.

Heezen, B. C., I. D. MacGregor, G. Z. Foreman, C. Z. Forristall, H. Hekel, R. Hesse, R. H. Hoskins, E. J. W. Jones, A. G. Kaneps, A. G. Krasheninnikov, H. Okanda, and M. H. Ruef, The post-Jurassic sedimentary sequence on the Pacific plate: A kinematic interpretation of diachronous deposits, in Initial Reports of the Deep Sea Drilling Project, 20, edited by B. C. Heezen et al., p. 725, U. S. Government Printing Office, Washington, D. C., 1973.

Houtz, R., J. Ewing, and X. Le Pichon, Velocity of deep-sea sediments from sonobuoy data, J. Geophys. Res., 73, 2615, 1968.

Houtz, R., J. Ewing, and P. Buhl, Seismic data from sonobuoy stations in the northern and equatorial Pacific, J. Geophys. Res., 75 5093, 1970.

Le Pichon, X., J. Ewing, and R. E. Houtz, Deep-sea sediment velocity determination made while reflection profiling, J. Geophys. Res., 73, 2597, 1968.

Neumann, E., Experimental recrystallization of dolomite and comparison of preferred orientations of calcite and dolomite in deformed rocks, J. Geol., 77, 426, 1969.

Nur, A., and G. Simmons, The effect of saturation on velocity in low-porosity rocks, Earth Planet. Sci. Lett., 7, 183, 1969.

Packham, G. H., and G. J. van der Lingen, Progressive carbonate diagenesis of Deep Sea Drilling Sites 206, 207, 208, and 210 in the southeast Pacific and its relationship to sediment physical properties and seismic reflectors, in Initial Reports of the Deep Sea Drilling Project, vol. 21, edited by R. E. Burns et al., p. 495, U. S. Government Printing Office, Washington, D. C., 1973.

Peselnick, L., and R. A. Robie, Elastic constants of calcite, J. Appl. Phys., 33, 2889, 1962.

Schlanger, S. O., and R. G. Douglas, Pelagic ooze-chalk-limestone transition and its implications for marine stratigraphy, Palagic Sediments: On Land and Under the Sea, Spec. Publ. 1, p. 117, Int. Ass. of Sedimentol., London, 1974.

Schreiber, E., J. Fox, and J. Petersen, Compressional sound velocities in semi-indurated sediments and basalts from DSDP Leg 11, in Hollister, D. C., J. I. Ewing et al., Initial Reports of the Deep Sea Drilling Project, 11, edited by C. D. Hollister et al., p. 723, U. S. Government Printing Office, Washington D. C., 1972.

Tucholke, B. E., N. T. Edgar, and R. E. Boyce, Physical properties of sediments and correlations with acoustic stratigraphy: Leg 35, Deep Sea Drilling Project, in Hollister, D. C., C. Craddock et al., Initial Reports of the Deep Sea Drilling Project, 35, edited by D. C. Hollister et al., p. 329, U. S. Government Printing Office, Washington, D. C., 1976.

van Andel, T. H., Cenozoic migration of the Pacific plate, northward shift of the axis of deposition, and palebathymetry of the central equatorial Pacific, Geology, 2, 507, 1974.

van der Lingen, G. J., and G. H. Packam, Relationships between diagenesis and physical properties of biogenic sediments of the Outong-Java Plateau (Sites 288, and 289, Deep Sea Drilling Project), in Initial Reports of the Deep Sea Drilling Project, vol. 30, U. S. Government Printing Office, Washington, D. C., 1975.

Wyllie, M. R. J., A. R. Gregory, and G. H. F. Gardner, An experimental investigation of factors affecting elastic wave velocities in porous media, Geophysics, 23, 459, 1958.

(Received March 1, 1978;
revised September 22, 1978;
accepted October 12, 1978).